II CONGRESSO NACIONAL DE ENGENHARIA MECÂNICA
II NATIONAL CONGRESS OF MECHANICAL ENGINEERING
12 a 16 de Agosto de 2002 - João Pessoa – PB

PRELIMINARY NUMERICAL SIMULATION OF THE TURBULENT FLOW AROUND A CIRCULAR CYLINDER

Angelo A. Mustto
e-mail: mustto@serv.com.ufrj.br

Gustavo C.R. Bodstein
Universidade Federal do Rio de Janeiro, Departamento de Engenharia Mecânica
Cx. P. 68503 - 21945-970 - Rio de Janeiro, RJ, BRASIL
e-mail: gustavo@serv.com.ufrj.br

Abstract. *In this paper we blend a Lagrangian algorithm of a subgrid-scale eddy-viscosity turbulence model with a Discrete Vortex Method algorithm to simulate the unsteady, two-dimensional, incompressible, high-Reynolds number flow around a circular cylinder. In this new algorithm, the no-penetration boundary condition is exactly satisfied by the application of the circle theorem, whereas the no-slip condition is explicitly enforced at a finite number of points on the cylinder surface. Both the no-slip and the conservation of circulation conditions are used together to determine the strength of the nascent Lamb vortices. The resulting system of algebraic equations is solved using the Least Squares Method. The convection step is carried out using a first-order Euler scheme. Using the Random Walk Method the subgrid-scale turbulence model is calculated as a turbulence diffusion step coupled with the viscous diffusion step of the algorithm. A long-time simulation is produced for a Reynolds number of* 10^5*. The time-averaged drag coefficient, the Strouhal number and the pressure coefficient are compared to experimental and numerical results available in the literature. The influences of the numerical parameters are also identified.*

Keywords: *Vortex methods, turbulence, wake, separation, circle theorem.*

1. INTRODUCTION

Accurate numerical simulations of incompressible flows around bluff bodies have been the subject of intense studies over the last decades. These flows are characterized by the occurrence of massive separation, where a region of irrotational flow surrounds a region of rotational flow containing vorticity from the boundary layer, the shear layers emanating from the separation points, and the wake downstream of the body. For low Reynolds numbers, the wake is laminar and steady, whereas, for large Reynolds numbers, the wake is turbulent and strongly unsteady.

In two-dimensional, incompressible, high-Reynolds number flows around a circular cylinder, the separation phenomenon associated with the existence of adverse pressure gradients on the cylinder surface occurs alternately on the top and bottom surfaces of the cylinder. This mechanism injects vorticity into the wake, causing vortex shedding and the formation of an oscillatory (Von-Kármán) wake, comprised of large pairs of vortices rotating in opposite directions and connected to each other by a vortex sheet. The alternating vortex shedding produces large pressure fluctuations on the surface, and the resulting lift and drag forces oscillate in time, the latter with twice the frequency of the former. For Reynolds numbers greater than about 200, three-dimensional effects become important, even for high aspect-ratio cylinders (Prasad and Williamson, 1997).

Due to the existence of large regions of concentrated vorticity, the (purely Lagrangian) Discrete Vortex (DV) method is particularly suitable to simulate flows around bluff bodies. This method essentially tracks the motion of individual vortices (or vorticity particles) using a Lagrangian description of the flow, which allows for the determination of the velocity field without the need of setting up a grid. A large number of different algorithms have been developed, and we may cite the reference papers by Chorin (1973), Sarpkaya and Schoaff (1979), Kuwuhara (1978), Porthouse and Lewis (1981), Kamemoto (1994) and Ogami and Ayano (1995). More detailed information can be found in the review paper by Sarpkaya (1994) and its references.

Mustto and Bodstein (2001) has recently developed an improved version of the DV method of Mustto et al (2000), which has proven to be very effective in calculating the main features of the flow around a circular cylinder. However, their mathematical model does not include any turbulence model for the smaller scales. Starting from the Eddy-Viscosity turbulence model proposed within the theory of Large-Eddy Simulation (LES) by Lesieur and Métais (1996), Hirata (2000) suggests a Lagrangian algorithm to model the subgrid-scale turbulence based on the Second-Order Velocity Structure Function, so that the effects of the turbulent diffusion on the overall boundary layer and wake dynamics can be calculated.

In this paper, we incorporate the Lagrangian algorithm proposed by Hirata (2000) of the turbulence model of Lesieur and Métais (1996) to the DV algorithm of Mustto and Bodstein (2001) to simulate the unsteady, two-dimensional, incompressible, high-Reynolds number flow around a circular cylinder. The DV method solves the flow for the large scales, whereas LES turbulence model takes the subgrid scales into account. Our main objective is to carry out a preliminary calculation to show that the overall performance of the simulation can be substantially improved when turbulence is taken into account. In our DV algorithm, the no-penetration boundary condition is exactly satisfied by the application of the Circle Theorem, whereas the no-slip condition is explicitly enforced on a finite number of points on the cylinder surface. In order to calculate the strength of the new Lamb vortices to be created in the flow every time step, the no-slip and the conservation of circulation conditions are used to form a system of algebraic equations that is solved using the Least Squares Method. The convection step is carried out using a first-order Euler scheme. The subgrid-scale turbulence is modeled as a turbulence diffusion step, implemented together with the viscous diffusion step of the algorithm using the Random Walk Method. We produce a long-time simulation of the flow around a circular cylinder, for a Reynolds number of 10^5, and show results for the temporal variation of the lift and drag coefficients. The time-averaged drag coefficient and the Strouhal number are compared to experimental and numerical results available in the literature. The influences of the numerical parameters are also identified.

2. MATHEMATICAL FORMULATION

Consider the flow around a circular cylinder immersed in an unbounded region with a uniform flow and freestream speed U. We assume the flow to be incompressible and two-dimensional, and the fluid to be Newtonian, with constant properties. The unsteady flow that develops has its origin at the separation that occurs on the cylinder surface, which generates an oscillatory wake downstream of the body. This flow is governed by the continuity and the Navier-Stokes equations, which can be rewritten using the theory of LES. In order to eliminate the fluctuations on subgrid scales, we separate the motion into large and small scales by considering the choice of a low-pass filter characterized by the function $\overline{G}$, defined for any scalar or vectorial flow quantity F as

$$\overline{F}(\boldsymbol{x},t) \equiv \int F(\boldsymbol{x}-\boldsymbol{y},t)\overline{G}(\boldsymbol{y})\, d\boldsymbol{y}\,. \tag{1}$$

Using Eq. (1), the filtered Navier-Stokes and continuity equations are

$$\frac{\partial \bar{u}_i}{\partial t} + \frac{\partial}{\partial x_j}\left(\overline{u_i u_j}\right) = -\frac{1}{\rho}\frac{\partial \bar{p}}{\partial x_i} + \frac{\partial}{\partial x_j}\left(\nu \frac{\partial \bar{u}_i}{\partial x_j}\right) , \tag{2}$$

$$\frac{\partial \bar{u}_i}{\partial x_i} = 0 , \tag{3}$$

where ρ and ν are the density and kinematic viscosity, respectively. Similarly to the Reynolds decomposition procedure, the second term on the left-hand side of Eq. (2) can be expanded decomposing $\bar{u}_i$ into $u_i = \bar{u}_i + u_i'$. With this equation, the convective term can be expanded out and the *subgrid-scale tensor* T_{ij}, defined as $T_{ij} \equiv \overline{u_i u_j} - \bar{u}_i \bar{u}_j$, can be introduced. Thus, Eq. (2) becomes

$$\frac{\partial \bar{u}_i}{\partial t} + \frac{\partial}{\partial x_j}\left(\bar{u}_i \bar{u}_j\right) = -\frac{1}{\rho}\frac{\partial \bar{p}}{\partial x_i} + \frac{\partial}{\partial x_j}\left(\nu \frac{\partial \bar{u}_i}{\partial x_j} - T_{ij}\right) . \tag{4}$$

In the equations above $\bar{u}_i$ is the filtered velocity field, and $\bar{p}$ is the filtered pressure field. We model the subgrid-scale tensor T_{ij} using the eddy-viscosity assumption (Boussinesq's hypothesis). We then write $T_{ij} = -2\nu_t \bar{S}_{ij}$, where $\bar{S}_{ij}$ is the deformation tensor of the filtered field defined by

$$\bar{S}_{ij} \equiv \frac{1}{2}\left(\frac{\partial \bar{u}_i}{\partial x_j} + \frac{\partial \bar{u}_j}{\partial x_i}\right) . \tag{5}$$

With these considerations and denoting the eddy viscosity by ν_t, Eq. (5) can be writen as

$$\frac{\partial \bar{u}_i}{\partial t} + \frac{\partial}{\partial x_j}\left(\bar{u}_i \bar{u}_j\right) = -\frac{1}{\rho}\frac{\partial \bar{p}}{\partial x_i} + 2\frac{\partial}{\partial x_j}\left[(\nu + \nu_t)\bar{S}_{ij}\right] , \tag{6}$$

The equations above and all the equations below can be nondimensionalized using U and the cylinder radius a. As a consequence, we define the molecular and the turbulence Reynolds numbers based on the cylinder diameter as $Re \equiv 2aU/\nu$ and $Re_t \equiv 2aU/\nu_t$, respectively. Therefore, Eq. (6), in dimensionless form, becomes

$$\frac{\partial \bar{u}_i}{\partial t} + \frac{\partial}{\partial x_j}\left(\bar{u}_i \bar{u}_j\right) = -\frac{\partial \bar{p}}{\partial x_i} + \frac{4}{Re_c}\frac{\partial \bar{S}_{ij}}{\partial x_j} , \tag{7}$$

$$\frac{\partial \bar{u}_i}{\partial x_i} = 0 , \tag{8}$$

where the combined Reynolds number Re_c is defined as $Re_c \equiv 2aU/(\nu + \nu_t)$.

In order to model the eddy viscosity, we use the model proposed by Lesieur & Métais (1996), which is based on the Smagorinsky model (1963). The model of Lesieur & Métais (1996) for ν_t expresses the local kinetic energy spectrum in terms of the Second-Order Structure Function (SF) of the filtered field, $\bar{F}_2$. In summary, the nondimensional eddy viscosity, *i.e.*, the turbulent Reynolds number, is given by

$$Re_t = \frac{2}{0.105\, C_K^{-3/2}\, \Delta \sqrt{\overline{F}_2(x_i, \Delta, t)}}, \tag{9}$$

where $C_K = 1.4$ is the Kolmogorov constant and Δ is a subgrid length scale. The dimensionless function $\overline{F}_2$, which gives a measure of the local intermittency of the turbulence, can be written as

$$\overline{F}_2(x_i, \Delta, t) = \overline{\left\| u_i(x,t) - u_i(x_i + r_i, t) \right\|^2}_{\|r_i\| = \Delta}, \tag{10}$$

In Eq. (10), the spatial filtering operator for $\overline{F}_2$ is applied to the local, instantaneous velocities $\boldsymbol{u}(\boldsymbol{x}+\boldsymbol{r}, t)$, which are calculated on the surface of a sphere centered at $\boldsymbol{x}$ and having a radius Δ. This model is suitable to be used in conjunction with the vortex method because the instantaneous velocity difference in Eq. (10) is associated with the turbulence fluctuations of subgrid scales.

Equations (7)-(10) form the system of partial differential equations to be solved. The flow is started impulsively from rest, and the boundary conditions can be expressed as

$$u_r \equiv \boldsymbol{u} \cdot \boldsymbol{e_r} = 0, \text{ at } r = 1 \tag{11a}$$

$$u_\theta \equiv \boldsymbol{u} \cdot \boldsymbol{e_\theta} = 0, \text{ at } r = 1, \tag{11b}$$

$$|\overline{u}_i| \to 1, \text{ as } r \to \infty. \tag{11c}$$

The dynamics of the fluid motion, governed by the boundary-value problem (7)-(11) can be alternatively studied using the vorticity transport equation, obtained by taking the curl of Eq. (7). For a 2-D flow this (scalar) equation can be written as

$$\frac{\partial \overline{\varpi}}{\partial t} + \overline{u}_j \frac{\partial \overline{\varpi}}{\partial x_j} = \frac{2}{Re_c} \frac{\partial^2 \overline{\varpi}}{\partial x_j \partial x_j}, \tag{12}$$

where $\overline{\varpi}$ is the only non-zero component of the vorticity vector (in a direction normal to the plane of the flow). Thus, we replace Eq. (7) by Eq. (12), and model the filtered vorticity field as a cloud of point vortices. Consequently, the velocity field can be constructed so as to automatically satisfy Eqs. (8), (11a) and (11c). Using the circle theorem (Milne-Thomson, 1955), a general expression for the complex velocity, dropping the overbar for convenience from this point on, is given by

$$u - iv = \left(1 - \frac{1}{z^2}\right) - \frac{i}{2\pi} \sum_{k=1}^{N_v} \frac{\Gamma_k}{z - z_k(t)} + \frac{i}{2\pi} \sum_{k=1}^{N_v} \frac{\Gamma_k}{z - z_{im,k}(t)}, \tag{13}$$

where: u and v are the components of $\boldsymbol{u}$ in the x and y directions, respectively; $i \equiv (-1)^{1/2}$; $z \equiv x + iy$ is the position of any point in the complex plane of the flow; z_k is the position of the k^{th}-point vortex with strength Γ_k, and $z_{im,k} \equiv 1/z_k^*$ is the position of its image at the inverse point of the image vortex with strength $\Gamma_{im,k} = -\Gamma_k$ (the symbol "*" denotes complex conjugate); N_v is the total number of vortices present in the flow (not considering their images).

The aerodynamic forces are calculated using the extended Blasius formula for unsteady flows (Milne-Thomson, 1955). This formula, applied to the problem under investigation, reduces to (Sarpkaya, 1994)

$$C_D + iC_L = -i \sum_{k=1}^{N_v} \Gamma_k \left[(u_k + iv_k) - (u_{im,k} + iv_{im,k}) \right], \tag{14}$$

where C_D and C_L are the drag and lift coefficients, respectively, and the velocities on the right-hand side of Eq. (6) are calculated at the k^{th}-vortex position and its image.

The pressure on the cylinder surface is obtained splitting the Navier-Stokes equations into

$$-\frac{\partial p}{\partial x_i} = \frac{\partial u_i}{\partial t}, \tag{15}$$

which can be integrated along the surface of the cylinder.

3. THE SOLUTION METHOD

3.1 The Vortex Method

The problem above is solved using the (Lagrangian) Discrete Vortex Method of Mustto and Bodstein (2001). This method is based on Eq. (12), and uses an algorithm that splits the convective-diffusive operator (Chorin, 1973) in the form

$$\frac{\partial \omega}{\partial t} + u_j \frac{\partial \omega}{\partial x_j} = 0, \tag{16a}$$

$$\frac{\partial \omega}{\partial t} = \frac{2}{Re_c} \frac{\partial^2 \omega}{\partial x_j \partial x_j} \ . \tag{16b}$$

In a real flow vorticity is generated on the body surface so as to satisfy the no-slip condition, Eq. (11b), and is transported by convection and diffusion into the flow according to Eq. (12). Our discrete vortex method uses discrete vortices to model the vorticity, whose transport at each time step is carried out in a sequence using a Lagrangian approach. The vortex generation process is accomplished following the scheme developed by Mustto and Bodstein (2001). Since the circle theorem guarantees that the no-penetration condition is satisfied exactly on the entire cylinder surface, we set up a linear system of algebraic equations that imposes the no-slip condition at specified points on the cylinder surface and the condition that the total circulation is conserved. If N vortices are generated at time t, the enforcement of the no-slip condition at N points on the cylinder surface yields a set of N equations and N unknowns (the strength of the new vortices). The condition that circulation is conserved adds an extra equation, and we end up with an overdetermined system of $N + 1$ equations and N unknowns. Mustto and Bodstein (2001) solves this system using the Projection and Least-Squares (LS) Approximations (Strang, 1988).

For the convective vorticity transport, governed by Eq. (16a), the motion of each vortex generated on the body surface is determined by integration of each vortex path equation. We employ the first-order Euler scheme to carry out the time-marching procedure. Therefore, the displacement of the k^{th}-vortex owing entirely to convection, $\Delta \boldsymbol{x}_{c,k}$, can be written as

$$\Delta \boldsymbol{x}_{c,k} \equiv \boldsymbol{x}_k(t + \Delta t) - \boldsymbol{x}_k(t) = \boldsymbol{u}_k \Delta t \ , \tag{17}$$

where $\boldsymbol{x}_k$ and $\boldsymbol{u}_k$ are the position and the velocity vectors of the k^{th}-vortex, respectively.

The process of viscous diffusion, governed by Eq. (16b), is simulated using the Random Walk Method (Lewis, 1991), where the random displacements of the k^{th}-vortex in the x and y directions owing entirely to viscous and turbulent diffusion, $\Delta x_{d,k}$ and $\Delta y_{d,k}$, are calculated from

$$\Delta x_{d,k} = \Delta r_k \cos(\Delta \theta_k) \ \text{ and } \ \Delta y_{d,k} = \Delta r_k \sin(\Delta \theta_k) \ , \tag{18a}$$

where

$$\Delta r_k = \left[8 Re_c^{-1} \Delta t \ln(1/P)\right]^{1/2}, \text{ and } \Delta\theta_k = 2\pi Q \ . \tag{18b}$$

In Eqs. (18b), P and Q are random numbers between 0 and 1 drawn from a uniform probability density distribution. The total vortex displacement is given by

$$\boldsymbol{x}_k(t+\Delta t) = \boldsymbol{x}_k(t) + \Delta\boldsymbol{x}_{c,k}(t) + \Delta\boldsymbol{x}_{d,k}(t). \tag{19}$$

In order to desingularize the point vortices we use Lamb vortices for $r \le \sigma$, where σ is the radius of the vortex core and r is the radial distance between the vortex center and the point in the flow where the induced velocity is calculated. Thus, the mathematical expression for the induced velocity of the k^{th}-vortex in the circumferential direction, $u_{\theta,k}$, is

$$u_{\theta,k} = \Gamma_k / 2\pi r \left\{1 - \exp\left[-5.0257\left(r^2/\sigma^2\right)\right]\right\}. \tag{20}$$

The time step Δt is calculated from $\Delta t = 2\pi k/N$, which is based on an estimate of the convective length and velocity scales of the flow. The parameter k represents an estimated upper bound on the maximum allowed convective step of a vortex.

The value of the distance ε off the cylinder surface where N new vortices are generated each time step is calculated based on a boundary layer model. We set the value of ε equal to the displacement thickness of a flat plate boundary layer, and we use classical results for both laminar and turbulent boundary layer displacement thicknesses (Lighthill, 1963). For high enough Reynolds numbers, the boundary layer thickness is much less than the cylinder radius, and the effect of the boundary layer curvature may be ignored. These models provide local values of the displacement thickness as a function the polar angle from the forward stagnation point, φ, and we can write

$$\varepsilon_L(\varphi) = 2.4336\left(\frac{\varphi}{Re}\right)^{1/2}, \text{ Laminar BL }, \tag{21a}$$

$$\varepsilon_T(\varphi) = 0.05313\left(\frac{\varphi^4}{Re}\right)^{1/5}, \text{ Turbulent BL }. \tag{21b}$$

We assume that transition occurs at a local Reynolds number based on the arc length of the cylinder surface equal to 5×10^5, which may be written in terms of a critical value for φ as $\varphi_{crit} = 10^6/Re$. This means that, for $Re > 3.18\times10^5$, Eq. (21a) must be used for $\varphi < \varphi_{crit}$ and Eq. (21b) for $\varphi > \varphi_{crit}$; otherwise, only Eq. (21a) must be used. These values of ε are also used to calculate the value of the vortex core σ, since we set σ equal to ε in the simulation.

The aerodynamic forces are obtained from Eq. (14). The time-averaged drag coefficient is computed over an integer number of cycles of oscillation (in the periodic steady-state regime) chosen from the time history of the lift coefficient. These cycles are also used to determine the Strouhal number (defined as $St = 2fa/U$) from the $C_L \times t$ graph, where f is the frequency (in Hz).

Integration of Eq. (15) along the body surface from the forward stagnation point, yields the following expression for the pressure coefficient at a point m of the cylinder surface

$$C_{p_m} = \left(p_{ref} + \frac{2}{\Delta t}\sum_{n=1}^{m}\Gamma_{v,n}\right) + 1 - p_s \ . \tag{22}$$

In Eq. (22), the $\Gamma_{v,n}$'s are the strengths of the vortices generated during a time step from position 1 up to position m, p_{ref} is an arbitrary reference pressure on the cylinder surface, and p_s is the pressure at the forward stagnation point. The time-averaged pressure field is computed for $t \geq 25$, that is, over the same cycles of oscillation as the force coefficients (approximately).

3.2 Implementation of the Turbulence Model into the Vortex Method

In order to implement the turbulence model of Lesieur and Métais (1996), we follow the numerical scheme proposed by Hirata (2000), which considers each vortex at a time as a reference vortex, all initially desingularized by the core radius σ. In a 2-D flow, the region where other vortices exert influence on the reference vortex is defined as a ring surrounding the reference vortex, with thickness $2\varepsilon_c$ from the radius σ. Thus, the ring area is defined by the radii $(\sigma \pm \varepsilon_c)$, as shown in Fig. (1). The value of the thickness ε_c is chosen as a percentage of σ, obtained from numerical experiments. Therefore, the second-order velocity structure function, given by Eq. (10), is modified as follows

$$\overline{F}_2 = \frac{1}{N_r} \sum_{k=1}^{N_r} \left\| \boldsymbol{u}(\boldsymbol{x},t) - \boldsymbol{u}(\boldsymbol{x}+\boldsymbol{r}_k,t) \right\|_k^2 \left(\frac{\sigma}{\boldsymbol{r}_k} \right)^{2/3} , \tag{23}$$

where N_r is the number of vortices in the ring, $\boldsymbol{r}_k$ is the distance between vortex k in the ring and the reference vortex, and $\boldsymbol{u}$ is the local instantaneous velocity of each vortex.

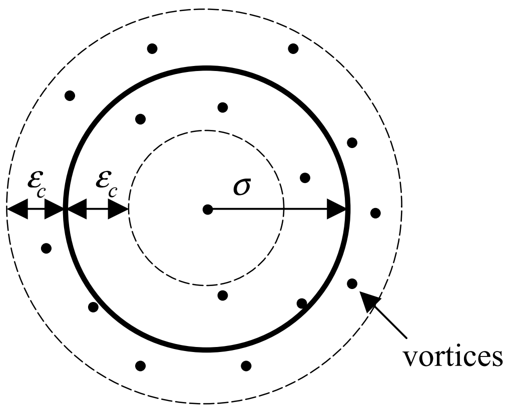

Figure 1. Implementation of the turbulence model.

With the Second-Order Structure Function, given by Eq. (23), the eddy viscosity (or the turbulent Reynolds number) is determined, and a modified core radius is calculated according to $\sigma_{mod}(t)$ = 6.340825 $(\Delta t/Re_c)^{1/2}$. The turbulent diffusion effects are taken into account through the temporal variation of $\sigma_{mod}(t)$ and the random walk scheme for the vorticity diffusion process.

4. RESULTS AND DISCUSSION

We now present results of our vortex method simulations carried out using the Lagrangian algorithm of the turbulence model described above, for a large value of the Reynolds number still in the subcritical regime: $Re = 10^5$. The numerical parameters we used in this simulation are: $k = 1$, $\Delta t = 0.1$, $N = 64$ and $\varepsilon_c = 0.90\sigma$. For this case the boundary layer is laminar, and only Eq. (21a) is used to calculate ε, the distance between the nascent vortices and the cylinder surface. The positions of the wake vortices are show in Fig. (2) at the last step of the computation ($t = 50$), where we can clearly observe the formation and shedding of large eddies in the wake. This process occurs alternately on the upper and lower surfaces of the cylinder. We can also visualize the vortex pairing process, where the vortices rotate in opposite directions and are connected to each other by a vortex sheet.

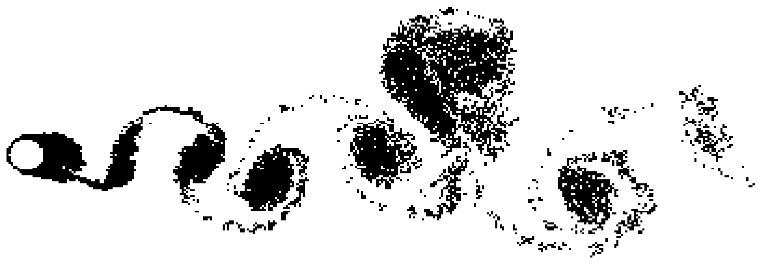

Figure 2. Position of the wake vortices at $t = 50$ for $Re = 10^5$;
numerical parameters: $N = 64$, $k = 1$, $\Delta t = 0.1$ and $\varepsilon_c = 0.90\sigma$.

The temporal history of the aerodynamic forces can be seen in Fig. (3a). The vortex shedding mechanism that characterizes the flow around a circular cylinder can be detected in the oscillations of the lift and drag coefficients. As soon as the numerical transient is over and the periodic steady-state regime is reached (from $t = 22$ on, approximately) the lift coefficient shows a large amplitude of oscillation, with a dimensionless frequency (Strouhal number) about twice the frequency of the drag coefficient, in accordance to the physics involved in the flow. The time-averaged drag coefficient and the Strouhal number, calculated over the last two cycles of oscillation of the lift coefficient curve (in the range $29.7 \leq t \leq 49.0$) are $C_D = 1.227$ and $St = 0.196$. These values are very close to the experimental values of Blevins (1984), that is, $C_D = 1.20$ and $St = 0.19$.

In order to illustrate the improvement on the calculation of a local variable obtained using the turbulence model, we plot in Fig. (3b) the time-averaged distribution of the pressure coefficient on the cylinder surface and compare it to the experimental results of Blevins (1984) and to the numerical results obtained with the same algorithm without the turbulence model. As shown, the agreement with the experimental results are much better when the turbulence model is used.

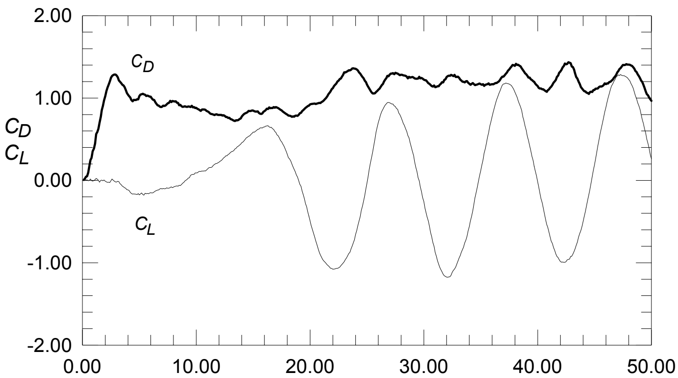

(a) variation of C_D and C_L with time;

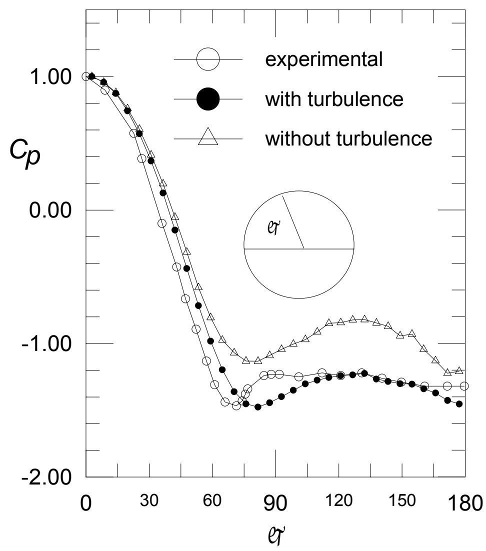

(b) C_p distribution with φ

Figure 3. Aerodynamic loads on a circular cylinder for $Re = 10^5$;
numerical parameters: $N = 64$, $k = 1$, $\Delta t = 0.1$ and $\varepsilon_c = 0.90\sigma$.

Table 1 summarizes a comparison of our results with experimental and numerical results obtained using different versions of the vortex method. As it can be seen, the agreement of our numerical results for the mean drag coefficient and the Strouhal number with the experimental results is very good, and they are better than the other numerical results. The values of C_D and St are slightly higher than the experimental ones due to three-dimensional effects that are present in the experiments but not in the 2-D simulations carried out here, for the Reynolds number used.

Table 1. Comparison with other results from the literature: $Re = 10^5$.

$Re = 10^5$	C_D	St
Blevins (1984) (experimental)	1.20	0.19
Ogami & Ayano (1995) (numerical)	1.10	---
Chorin (1973) (numerical)	1.07	---
Mustto et al (2000) (numerical)	1.22	0.22
Mustto and Bodstein (2001) (numerical)	1.07	0.20
Present simulation	1.23	0.20

Table 2 shows the effect of N and Δt on the results obtained also from simulations for $Re = 10^5$. The calculated values of C_D (integrated from $t = 0$ to 50) and St (obtained from the C_L temporal oscillation) as a function of three values of N and Δt indicate that, as Δt decreases, keeping N constant, the values of C_D and St increases. On the other hand, when N increases, keeping Δt constant, the value of C_D increases and the value of St decreases towards the experimental values, given in Table 1. The effect of N on the distribution of C_p on the cylinder surface is depicted in Fig. 4. The results also show a significant improvement as N increases, since the numerical C_p distribution approaches the experimental distribution.

Table 2. Variation of C_D and St with N and Δt; $Re=10^5$

N	Δt	C_D	St
16	0,20	0,266	---*
16	0,15	0,482	0,201
16	0,10	0,707	0,220
32	0,20	0,560	0,167
32	0,15	0,829	0,202
32	0,10	0,981	0,201
64	0,20	0,759	0,156
64	0,15	0,923	0,171
64	0,10	1,072	0,196

* C_L does not oscillate and St cannot be computed.

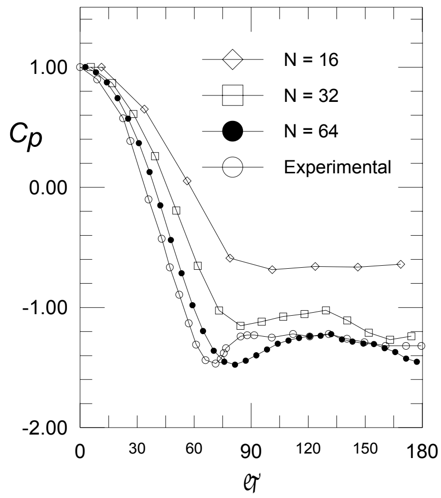

Figure 4: C_p distribution with φ as a function of N, for $\Delta t = 0.10$ and $Re=10^5$.

5. CONCLUSIONS

A new algorithm comprised of a Lagrangian Discrete Vortex Method and a new Lagrangian scheme for an eddy-viscosity turbulence model is used to simulate the unsteady, two-dimensional, incompressible, high-Reynolds number flow around a circular cylinder.

Preliminary calculations show that the resulting algorithm is capable of predicting very well the main quantities inherent to the flow. The use of a turbulence model improves the performance of the algorithm tested and produces better results than previous Lagrangian vortex method algorithms that do not use a turbulence model. The evolution of the wake is calculated correctly and the aerodynamic forces are also obtained accurately. The calculated values of the drag coefficient and the Strouhal number are closer to the experimental data than other numerical results available in the literature, for the high value of the Reynolds number investigated. The effect of the number of nascent vortices and time step has been identified. However, the algorithm needs to be more thoroughly explored to evaluate its performance for a wide range of values of the Reynolds number.

6. ACKNOWLEDGEMENTS

The authors would like to acknowledge the Brazilian National Council for Scientific and Technological Development (CNPq), under grants no. 521260/94-9, 141851/98-8 and 474904/01-6, for the financial support of this project.

7. REFERENCES

Blevins, R. D., "Applied Fluid Dynamics Handbook", Van Nostrand Reinhold Co., 1984.

Chorin, A. J., "Numerical Study of Slightly Viscous Flow", Journal of Fluid Mechanics, Vol. 57, 1973, pp. 785-796.

Hirata, M. H., "O Método de Vórtices com Modelagem da Turbulência", CONEM 2000 - Congresso Nacional de Engenharia Mecânica, Natal, RN, 07-11 Agosto, 2000.

Kamemoto, K., "Development of Vortex Methods for Grid-Free Lagrangian Direct Numerical Simulation", Proceedings of the 3th. JSME-KSME Fluids Engineering Conference, July 25-27, Sendai, Japan, 1994.

Kuwahara, K., "Study of Flow Past a Circular Cylinder by an Inviscid Model", Journal of Physical Society of Japan, Vol. 45, Jan 1978, pp. 292-297.

Lewis, R. I., "Vortex Element Methods for Fluid Dynamic Analysis of Engineering Systems", Cambridge University Press, Cambridge, 1991.

Lesieur, M., Métais, O., 1996, "New Trends in Large-Eddy Simulations of Turbulence", Annual Review of Fluid Mechanics, Vol. 28, pp. 45-82

Lighthill, M. J., "Introduction. Boundary Layer Theory", in Laminar Boundary Layers, Edited by L. Rosenhead, Dover, 1963.

Milne-Thomson, L. M., "Theoretical Hydrodynamics", MacMillan & Co., 1955.

Mustto, A. A., Bodstein, G. C. R., and Hirata, M. H, "Vortex Method Simulation of the Flow Around a Circular Cylinder", AIAA Journal, Vol. 38, No. 6, 2000, pp.1100-1102.

Mustto, A. A., and Bodstein, G. C. R., "Improved Vortex Method for the Simulation of the Flow Around Circular Cylinders", AIAA Paper 2001-2643, 15th AIAA Computational Fluid Dynamics Conference, Anaheim, California, EUA, June 11-14, 2001.

Ogami, Y., and Ayano, Y., "Flows around a Circular Cylinder Simulated by the Viscous Vortex Model - the Diffusion Velocity Method", Computational Fluid Dynamics Journal, Vol. 4, No. 3, Oct 1995, pp. 383-399.

Porthouse, D. T. C., and Lewis, R. I., "Simulation of Viscous Diffusion for Extension of the Surface Vorticity Method to Boundary Layer and Separated Flows", Journal Mechanical Engineering Science, Vol. 23, Aug 1981, pp. 157-167.

Prasad, A., and Williamson, C. H. K., "Three-Dimensional Effects in Turbulent Bluff-Body Wakes", Journal of Fluid Mechanics, Vol. 343, 1997, pp. 235-265.

Press, W.H., Flannery, B.P., Teukolsky, S.A. & Vetterling, W.T., "Numerical Recipes - the Art of Scientific Computing (Fortran Version)", Cambridge University Press, 1989.

Sarpkaya, T. and Schoaff, R. L "Inviscid Model of Two-Dimensional Vortex Shedding by a Circular Cylinder", AIAA Journal, Vol. 17, Nov 1979, pp. 1193-1200.

Sarpkaya, T., "Vortex Element Methods for Flow Simulation", in Advances in Applied Mechanics, Academic Press, Vol. 31, 1994, pp. 113-247.

Smagorinsky, J., 1963, "General Circulation Experiments with the Primitive Equations", *Mon. Weath. Rev.* 91, 99-164.

Strang, G., "Linear Algebra and Its Applications", Harcourt Brace Jovanovich, 3rd. Edition, 1988.